Title
Measurements of absolute concentrations of NADH in cells using the phasor FLIM method

Journal
Biomedical Optics Express, 7(7)

ISSN
2156-7085

Authors
Ma, Ning
Digman, Michelle A
Malacrida, Leonel
et al.

Publication Date
2016-07-01

DOI
10.1364/boe.7.002441

Biomedical Optics EXPRESS

Measurements of absolute concentrations of NADH in cells using the phasor FLIM method

Ning Ma, Michelle A. Digman, Leonel Malacrida, and Enrico Gratton*

Laboratory for Fluorescence Dynamics, Biomedical Engineering Department,University of California, Irvine, CA 92697, USA

**egratton22@gmail.com*

Abstract: We propose a graphical method using the phasor representation of the fluorescence decay to derive the absolute concentration of NADH in cells. The method requires the measurement of a solution of NADH at a known concentration. The phasor representation of the fluorescence decay accounts for the differences in quantum yield of the free and bound form of NADH, pixel by pixel of an image. The concentration of NADH in every pixel in a cell is obtained after adding to each pixel in the phasor plot a given amount of unmodulated light which causes a shift of the phasor towards the origin by an amount that depends on the intensity at the pixel and the fluorescence lifetime at the pixel. The absolute concentration of NADH is obtained by comparison of the shift obtained at each pixel of an image with the shift of the calibrated solution.

OCIS codes: (180.0180) Microscopy; (180.2520) Fluorescence microscopy.

References and links

1. D. J. Bonda, H. G. Lee, A. Camins, M. Pallàs, G. Casadesus, M. A. Smith, and X. Zhu, "The sirtuin pathway in ageing and Alzheimer disease: Mechanistic and therapeutic considerations," Lancet Neurol. **10**(3), 275–279 (2011).
2. B. Chance, "Mitochondrial NADH redox state, monitoring discovery and deployment in tissue," Methods Enzymol. **385**, 361–370 (2004).
3. M. R. Kasimova, J. Grigiene, K. Krab, P. H. Hagedorn, H. Flyvbjerg, P. E. Andersen, and I. M. Møller, "The free NADH concentration is kept constant in plant mitochondria under different metabolic conditions," Plant Cell **18**(3), 688–698 (2006).
4. A. Mayevsky and B. Chance, "A new long-term method for the measurement of NADH fluorescence in intact rat brain with chronically implanted cannula," Adv. Exp. Med. Biol. **37**, 239–244 (1973).
5. N. Plotegher, C. Stringari, S. Jahid, M. Veronesi, S. Girotto, E. Gratton, and L. Bubacco, "NADH fluorescence lifetime is an endogenous reporter of α-synuclein aggregation in live cells," FASEB J. **29**(6), 2484–2494 (2015).
6. C. Stringari, R. A. Edwards, K. T. Pate, M. L. Waterman, P. J. Donovan, and E. Gratton, "Metabolic trajectory of cellular differentiation in small intestine by Phasor Fluorescence Lifetime Microscopy of NADH," Sci. Rep. **2**, 568 (2012).
7. C. Stringari, J. L. Nourse, L. A. Flanagan, and E. Gratton, "Phasor fluorescence lifetime microscopy of free and protein-bound NADH reveals neural stem cell differentiation potential," PLoS One **7**(11), e48014 (2012).
8. K. Torno, B. K. Wright, M. R. Jones, M. A. Digman, E. Gratton, and M. Phillips, "Real-time analysis of metabolic activity within Lactobacillus acidophilus by phasor fluorescence lifetime imaging microscopy of NADH," Curr. Microbiol. **66**(4), 365–367 (2013).
9. B. K. Wright, L. M. Andrews, M. R. Jones, C. Stringari, M. A. Digman, and E. Gratton, "Phasor-FLIM analysis of NADH distribution and localization in the nucleus of live progenitor myoblast cells," Microsc. Res. Tech. **75**(12), 1717–1722 (2012).
10. B. K. Wright, L. M. Andrews, J. Markham, M. R. Jones, C. Stringari, M. A. Digman, and E. Gratton, "NADH distribution in live progenitor stem cells by phasor-fluorescence lifetime image microscopy," Biophys. J. **103**(1), L7–L9 (2012).
11. J. C. Waters, "Accuracy and precision in quantitative fluorescence microscopy," J. Cell Biol. **185**(7), 1135–1148 (2009).
12. D. M. Jameson, V. Thomas, and D. M. Zhou, "Time-resolved fluorescence studies on NADH bound to mitochondrial malate dehydrogenase," Biochim. Biophys. Acta **994**(2), 187–190 (1989).
13. J. R. Lakowicz, H. Szmacinski, K. Nowaczyk, and M. L. Johnson, "Fluorescence lifetime imaging of free and protein-bound NADH," Proc. Natl. Acad. Sci. U.S.A. **89**(4), 1271–1275 (1992).

#263167 Received 14 Apr 2016; revised 19 May 2016; accepted 19 May 2016; published 1 Jun 2016

14. B. Kierdaszuk, H. Malak, I. Gryczynski, P. Callis, and J. R. Lakowicz, "Fluorescence of reduced nicotinamides using one- and two-photon excitation," Biophys. Chem. **62**(1-3), 1–13 (1996).
15. S. A. Sánchez, T. L. Hazlett, J. E. Brunet, and D. M. Jameson, "Aggregation states of mitochondrial malate dehydrogenase," Protein Sci. **7**(10), 2184–2189 (1998).
16. M. C. Skala, K. M. Riching, D. K. Bird, A. Gendron-Fitzpatrick, J. Eickhoff, K. W. Eliceiri, P. J. Keely, and N. Ramanujam, "In vivo multiphoton fluorescence lifetime imaging of protein-bound and free nicotinamide adenine dinucleotide in normal and precancerous epithelia," J. Biomed. Opt. **12**(2), 024014 (2007).
17. M. C. Skala, K. M. Riching, A. Gendron-Fitzpatrick, J. Eickhoff, K. W. Eliceiri, J. G. White, and N. Ramanujam, "In vivo multiphoton microscopy of NADH and FAD redox states, fluorescence lifetimes, and cellular morphology in precancerous epithelia," Proc. Natl. Acad. Sci. U.S.A. **104**(49), 19494–19499 (2007).
18. P. P. Provenzano, K. W. Eliceiri, and P. J. Keely, "Multiphoton microscopy and fluorescence lifetime imaging microscopy (FLIM) to monitor metastasis and the tumor microenvironment," Clin. Exp. Metastasis **26**(4), 357–370 (2009).
19. M. Skala and N. Ramanujam, "Multiphoton redox ratio imaging for metabolic monitoring in vivo," Methods Mol. Biol. **594**, 155–162 (2010).
20. T. S. Blacker, Z. F. Mann, J. E. Gale, M. Ziegler, A. J. Bain, G. Szabadkai, and M. R. Duchen, "Separating NADH and NADPH fluorescence in live cells and tissues using FLIM," Nat. Commun. **5**, 3936 (2014).
21. A. Venkateswaran, K. R. Sekhar, D. S. Levic, D. B. Melville, T. A. Clark, W. M. Rybski, A. J. Walsh, M. C. Skala, P. A. Crooks, E. W. Knapik, and M. L. Freeman, "The NADH oxidase ENOX1, a critical mediator of endothelial cell radiosensitization, is crucial for vascular development," Cancer Res. **74**(1), 38–43 (2014).
22. S. Kalinina, J. Breymayer, P. Schäfer, E. Calzia, V. Shcheslavskiy, W. Becker, and A. Rück, "Correlative NAD(P)H-FLIM and oxygen sensing-PLIM for metabolic mapping," J. Biophotonics **2016**, 297 (2016).
23. C. Kang, H. L. Wu, C. Zhou, S. X. Xiang, X. H. Zhang, Y. J. Yu, and R. Q. Yu, "Quantitative fluorescence kinetic analysis of NADH and FAD in human plasma using three- and four-way calibration methods capable of providing the second-order advantage," Anal. Chim. Acta **910**, 36–44 (2016).
24. A. V. Meleshina, V. V. Dudenkova, M. V. Shirmanova, V. I. Shcheslavskiy, W. Becker, A. S. Bystrova, E. I. Cherkasova, and E. V. Zagaynova, "Probing metabolic states of differentiating stem cells using two-photon FLIM," Sci. Rep. **6**, 21853 (2016).
25. Q. Yu and A. A. Heikal, "Two-photon autofluorescence dynamics imaging reveals sensitivity of intracellular NADH concentration and conformation to cell physiology at the single-cell level," J. Photochem. Photobiol. B **95**(1), 46–57 (2009).
26. M. A. Digman, V. R. Caiolfa, M. Zamai, and E. Gratton, "The phasor approach to fluorescence lifetime imaging analysis," Biophys. J. **94**(2), L14–L16 (2008).
27. C. Stringari, A. Cinquin, O. Cinquin, M. A. Digman, P. J. Donovan, and E. Gratton, "Phasor approach to fluorescence lifetime microscopy distinguishes different metabolic states of germ cells in a live tissue," Proc. Natl. Acad. Sci. U.S.A. **108**(33), 13582–13587 (2011).
28. M. S. Levin, B. Locke, N. C. Yang, E. Li, and J. I. Gordon, "Comparison of the ligand binding properties of two homologous rat apocellular retinol-binding proteins expressed in Escherichia coli," J. Biol. Chem. **263**(33), 17715–17723 (1988).
29. R. D. Fugate and P. S. Song, "Spectroscopic characterization of beta-lactoglobulin-retinol complex," Biochim. Biophys. Acta **625**(1), 28–42 (1980).
30. R. Datta, A. Alfonso-García, R. Cinco, and E. Gratton, "Fluorescence lifetime imaging of endogenous biomarker of oxidative stress," Sci. Rep. **5**, 9848 (2015).
31. D. A. Kolb and G. Weber, "Quantitative demonstration of the reciprocity of ligand effects in the ternary complex of chicken heart lactate dehydrogenase with nicotinamide adenine dinucleotide oxalate," Biochemistry **14**(20), 4471–4476 (1975).
32. Q. Zhang, D. W. Piston, and R. H. Goodman, "Regulation of corepressor function by nuclear NADH," Science **295**(5561), 1895–1897 (2002).
33. A. A. Heikal, "Intracellular coenzymes as natural biomarkers for metabolic activities and mitochondrial anomalies," Biomarkers Med. **4**(2), 241–263 (2010).
34. R. A. Neher and E. Neher, "Applying spectral fingerprinting to the analysis of FRET images," Microsc. Res. Tech. **64**(2), 185–195 (2004).
35. J. Wlodarczyk, A. Woehler, F. Kobe, E. Ponimaskin, A. Zeug, and E. Neher, "Analysis of FRET signals in the presence of free donors and acceptors," Biophys. J. **94**(3), 986–1000 (2008).
36. A. Woehler, J. Wlodarczyk, and E. Neher, "Signal/noise analysis of FRET-based sensors," Biophys. J. **99**(7), 2344–2354 (2010).
37. A. Zeug, A. Woehler, E. Neher, and E. G. Ponimaskin, "Quantitative intensity-based FRET approaches--a comparative snapshot," Biophys. J. **103**(9), 1821–1827 (2012).
38. A. D. Hoppe, B. L. Scott, T. P. Welliver, S. W. Straight, and J. A. Swanson, "N-way FRET microscopy of multiple protein-protein interactions in live cells," PLoS One **8**(6), e64760 (2013).
39. B. L. Scott and A. D. Hoppe, "Three-dimensional reconstruction of three-way fret microscopy improves imaging of multiple protein-protein interactions," PLoS One **11**(3), e0152401 (2016).
40. R. A. Colyer, C. Lee, and E. Gratton, "A novel fluorescence lifetime imaging system that optimizes photon efficiency," Microsc. Res. Tech. **71**(3), 201–213 (2008).

#263167 Received 14 Apr 2016; revised 19 May 2016; accepted 19 May 2016; published 1 Jun 2016

41. D. M. Jameson and G. Mocz, "Fluorescence polarization/anisotropy approaches to study protein-ligand interactions: effects of errors and uncertainties," Methods Mol. Biol. **305**, 301–322 (2005).

1. Introduction

The accurate determination of concentration of common cellular metabolites is fundamentally important for understanding cellular metabolism and changes in metabolism due to cell cycle, stress, cancer, diabetes and neurodegenerative diseases [1–10]. In fluorescence microscopy, the measurement of the concentration of a fluorescent molecule in a cell is commonly achieved by a calibration procedure in which the fluorescence signal is measured for a known concentration of the substance in a homogeneous solution and then this signal is compared with the signal from the fluorophore in the cell. This method works when the intensity of the fluorescent substance is greater than any fluorescent background, when there is only one fluorophore in the sample and when there is no change of the quantum yield of the fluorophore from the solution used for calibration and the quantum yield of the fluorophore in the cell.

NADH (the reduced form of the nicotinamide adenine dinucleotide) is an intrinsic fluorescent, common and abundant co-enzyme related to metabolism found in every living cell. For this specific fluorescence substance, a simple calibration procedure as described above cannot be applied because NADH exists in at least two forms, in the free state, with a lifetime of approximately 0.4ns (low quantum yield) and in the protein bound state, where the quantum yield could be much higher. Unless we know the relative amount of the free and bound form of NADH in every pixel of the image, the simple calibration procedure based on comparison with the intensity of a calibrated solution [11] cannot be applied because the quantum yield is not the same as in the solution. Furthermore, there is a very small spectral difference between the free and bound form of NADH. The lifetime of the pure bound form of NADH is not easy to obtain directly from biological samples since the NADH concentration is large and the concentrations of enzymes is low in typical cells. Lifetime values reported in the literature for NADH range from 1.4 to 9 ns possibly due to a combination of bound and free forms and due to protein aggregation or sequestering [5, 6, 9, 10, 12–24]. This very large range implies that the specific protein binding to NADH could strongly affect the quantum yield of NADH. Methods based on the determination of exponential components in the decay associated with different molecular species have been proposed to yield the concentration of NADH in cells [25] but methods based on the fit-free phasor approach to the best of our knowledge have not been described.

In this paper we propose a graphical method that will resolve the issue of the two different quantum yields of NADH and provide absolute values of the NADH concentration using a single calibration with a solution of free NADH of known concentration. The proposed method makes use of the phasor representation of the fluorescence lifetime and of a graphical solution of the changes of the phasor position at each pixel of an image when a given amount of unmodulated light is added to the entire image [26]. The addition of light to the lifetime decay does not require the physical addition of light in the detection pathway. In fact, it can be achieved mathematically by adding a constant value to the decay at each pixel. To our knowledge, this is the first time that such graphical approach is proposed.

The proposed graphical approach could be applied to any combination of molecular species in a pixel provided that the quantum yield of each species is known. Although in this paper we describe the determination of absolute concentration of NADH, the same approach could be applied to the determination of other substances such as retinoic acid, folate and flavins that have different quantum yield in cell with respect to solutions [27–29].

#263167 Received 14 Apr 2016; revised 19 May 2016; accepted 19 May 2016; published 1 Jun 2016

2. The phasor method to determine absolute concentrations of NADH in cells

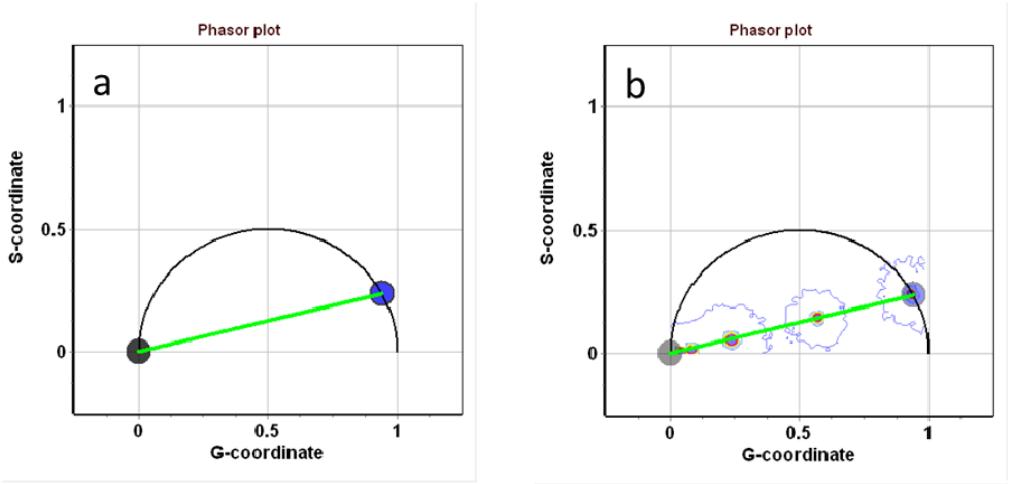

Fig. 1. a) Phasor representation of a single exponential component on the universal circle (blue circle) and a component of unmodulated light at the origin (black circle). b) Experimental value of the free-NADH lifetime (blue circle). When different amounts of unmodulated light are added to the sample, the phasor position moves towards the origin according to phasor addition. In this figure, we use a physical source of unmodulated light to shift the position of the phasor of the free-NADH. A mathematical addition of a constant to each pixel of the decay gives the same plot.

In Fig. 1(a) we schematically show the principle of the method. The blue circle indicates the phasor position of free-NADH, which could be obtained experimentally as shown in Fig. 1(b). The phasor position of the free-NADH lies on the universal circle hence the lifetime of this species is well approximated by a single exponential. Since the fluorescence lifetime is independent of a constant intensity value to the measured decay, the phasor of this unmodulated light is at the origin (Fig. 1, black circle). The constant intensity could be an external light source or, more conveniently, we can add a constant number to the record of the decay. In either case we will call it measurement with "external light added". After the phasor transformation, there is no difference whether the decay was measured in the frequency domain or in the time domain using the popular TCSPC [26]. In either case the phasor of the solution of free-NADH moves toward the origin. For the measurements shown in this paper, all measurements were obtained with the TCSPC card as described in the method section.

As we increase the amount of the unmodulated light added, the phasor of the free-NADH solution moves towards the origin due to phasor addition [26], as shown experimentally in Fig. 1(b). However, the amount of shift toward the origin depends on the relative intensity of the free-NADH solution and the amount of external light added. The intensity depends on the concentration of the solution and the quantum yield of the fluorophore. Figure 1(b) shows a series of measurements in which a solution of 1mM NADH is added with an increasing amount of unmodulated light L. In this case we actually added an external light source, but the same effect could be obtained if we "mathematically" add a constant to the measured decay. For a given amount of light added, the shift toward the origin depends on the total fluorescence of the solution of NADH (our calibration solution). Therefore by measuring the shift for a given amount of "external light added" we can determine the concentration of an unknown solution by comparison with the calibrated solution (Fig. 1(b)). Specifically, the distance (M) of the blue circle from the origin can be expressed in terms of the external light intensity L and the amount F of fluorescence emitted by a known concentration of NADH

#263167 Received 14 Apr 2016; revised 19 May 2016; accepted 19 May 2016; published 1 Jun 2016

$$M = \frac{L}{L+F} \tag{1}$$

The value of M, which is the modulation of the phasor in Fig. 1(b) can be measured with high precision for each value of L added. In this paper we will use the projection of M on the x-axis that we call the g-coordinate, as done in most of the papers using phasors.

In Fig. 2 we show the experimental graph of the g-coordinate calculated using the following formula

$$g = g_0 \frac{L}{L+F} \tag{2}$$

where g0 is the g-coordinate of the calibration solution without external light added and the values of F and L are obtained directly from the average of the intensity of the calibrated solution and from the amount of "external light added", respectively, as defined in Eq. (1). Since the amount of "external light added" is known, the only experimental quantity we need is the intensity F of the free-NADH solution used for calibration.

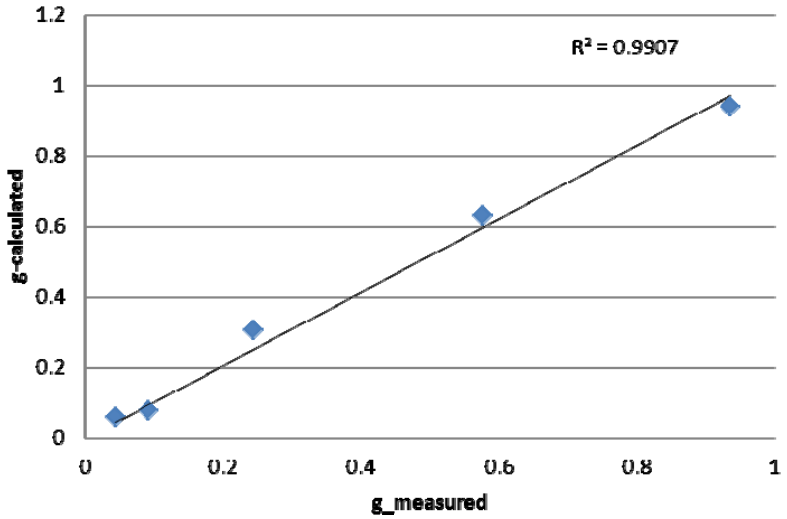

Fig. 2. Relationship between the experimental value of the g coordinate of the phasor plot and the value of g calculated using Eq. (2), for different amounts of external light L

While in Fig. 2 we show several points, only one point with "external light added" needs to be obtained along the line of calibration since the g0 value is directly measured and the calibration line must pass through the origin. This single point along the line in Fig. 2 will be the calibration point we will use to determine the concentration of an unknown sample. Of course, the same amount of "external light added" should be used for the measurement of the unknown sample.

3. Linear combination of free and bound NADH

In this work we focused on the measurement of the absolute concentration of NADH in every pixel of an image of a cell. All of the measurements were done using a 2-photon laser excitation set to 740nm and the emission was collected with emission bandpass filter (460/40 nm) to select the emission of NADH. Previous measurements in our lab have shown that the

#263167 Received 14 Apr 2016; revised 19 May 2016; accepted 19 May 2016; published 1 Jun 2016

NADH lifetime when bound to the LDH (Lactate Dehydrogenase) enzyme is ~3.4ns [27, 30]. For this work, we repeated the measurements to obtain the value of the NADH lifetime bound to LDH and the value of the free form of NADH in solution. We found that our measured lifetimes are in full agreement with previous measurements. In Fig. 3(a), the phasor of NADH for a combination of free and bound NADH in a given pixel should fall along the green line in Fig. 3(a) from the blue (free NADH) to the red circles (bound NADH). The phasor clusters in Fig. 3(a) correspond to experimental values determined for this work using the same instrument used for all measurements reported here.

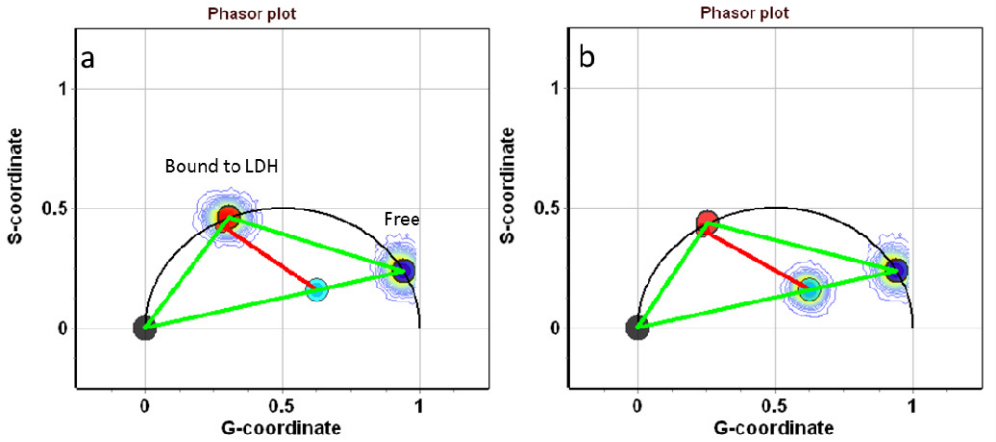

Fig. 3. Linear combination of free and bound NADH. a) The blue and red circles indicate the phasor position for free and bound NADH, respectively. Underlying the circles is the experimentally determined phasors of the free and bound form of NADH. Every possible combination in a pixel of free and bound NADH will be on the green line joining the phasor of the free and bound NADH. b) Upon addition of the external light, the phasor of the free and bound NADH moves toward the origin, but in different amounts as indicated by the red line. However, all points of the shifted red line have the same concentration equal to the concentration of the calibration solution since the solution phasor has moved by a given amount along the line of linear combination with the phasor at the origin.

Along this line every point represents a different linear combination of free and bound NADH. As the "external light" is added, the entire line of linear combination will move according to the changes of position of the red and blue circles, respectively. Since the red circle represents molecules with high quantum yield (long lifetime) while the blue circle represents molecules with low quantum yield (short lifetime), the two points will move by different amounts as shown in Fig. 3(b), red line. All points along the red line in Fig. 3(b) have the same concentration which is equal to the concentration of the calibration NADH solution. However, if some pixels in the image contain a smaller amount of NADH (than the calibration solution), they will move further toward the origin than pixels where NADH is more concentrated. From this shift we can determine the absolute NADH concentration in every pixel of the image.

4. Determining the absolute concentration of NADH in cells

Figure 4(a) shows the autofluorescence of a CHO-K1 cell by two-photon excitation at 740 nm, with an emission filter at 460/40 nm and the corresponding phasor plot is show in Fig. 4(b).

#263167 Received 14 Apr 2016; revised 19 May 2016; accepted 19 May 2016; published 1 Jun 2016

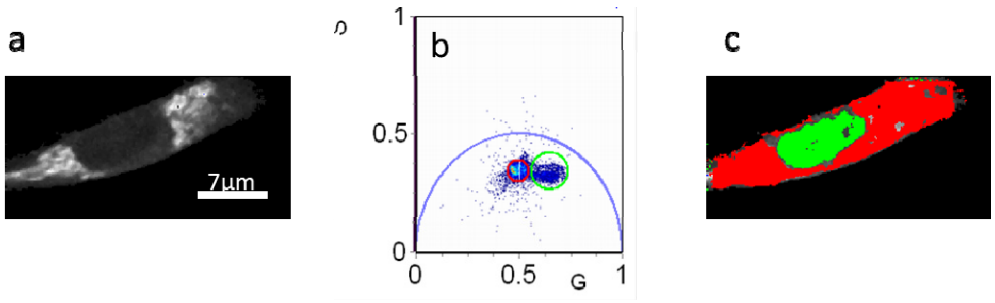

Fig. 4. a) Intensity image of a CHO-K1 cell in a gray scale. b) The phasor plot shows two characteristic clusters shown by the red and green cursors. c) All pixels in the red cursor are painted in red and all pixels in the green cursor are painted in green.

In the phasor plot of Fig. 4(b) there are two major clusters, one highlighted by the green cursor corresponding to shorter lifetime values in the cell nucleus and the other cluster highlighted by the red cursor with longer lifetime values and painted in red corresponding to pixels in the cytoplasm (Fig. 4(c)). However, in the cytoplasm there are regions of equal lifetime but very different intensities (Fig. 4(a)). Based on intensity only we cannot tell if the concentration of NADH in the cytoplasm is similar in every pixel and different from the nucleus. It could be that the concentration is the same but the quantum yield is very different in different parts of the cell.

When the external light is added to every pixel of the image, the image contrast changes (Fig. 5(a)) and the entire phasor distribution moves toward the origin (Fig. 5(b)). It is easy to see that some pixels move more than others toward the origin, indicating different NADH concentration in these pixels.

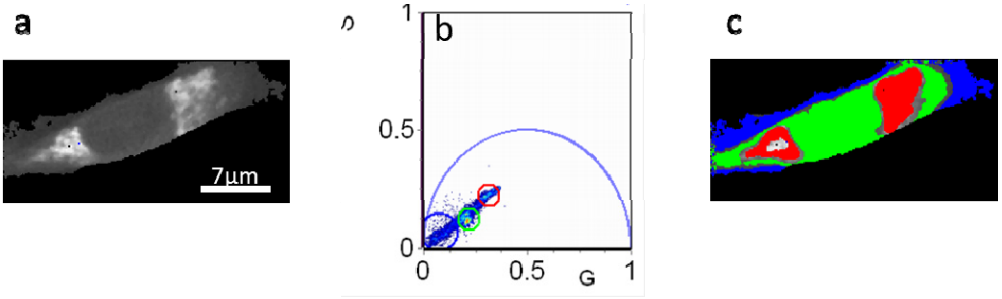

Fig. 5. a) Same CHO-K1 cell as in Fig. 4 with external light added. Note that the contrast of the image is quite different from Fig. 4(a). b) Comparing panels b in Figs. 4 and 5 we can determine that some pixels of the image have moved more than others toward the origin, indicating a different concentration of NADH in those pixels. c) Same image colored according the cursors selection in panel b.

To obtain the NADH concentration in the various parts of the cell, we use the calibrated phasor plot for a given intensity of the external light (Fig. 3(b)). In Fig. 6 we show how to use the calibration to display the concentration of NADH of the various pixels of the image.

#263167 Received 14 Apr 2016; revised 19 May 2016; accepted 19 May 2016; published 1 Jun 2016

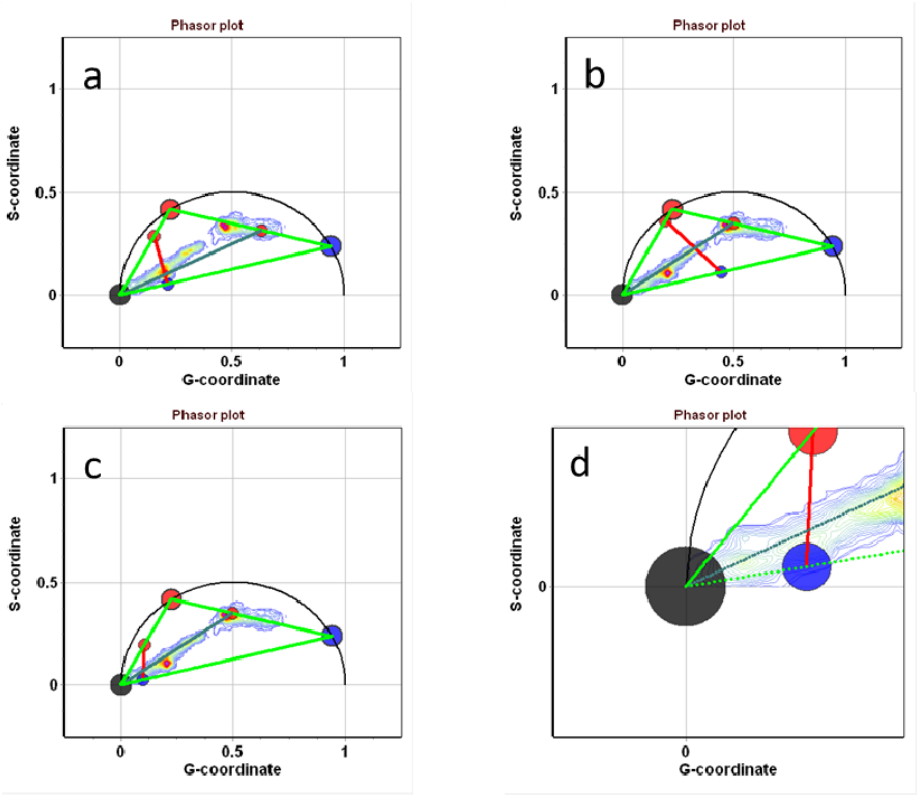

Fig. 6. The cell phasor plots are shown in the background of each of the panels in this figure together with the phasor plot obtained with a certain amount of external light added. a) The amount of light added moves the red line to the position shown in panel a). All pixels with phasors along the red line have equal concentration (0.29 mM). These pixels correspond to the nucleus and part of the cytoplasm of the cell as shown in Fig. 5(b). b) Using less external light, the red line moves away from the origin. All points along this line have a concentration of 0.89mM. These points are selected by the red cursor in Fig. 5(b) and they map to the brighter pixels in the cytoplasm. c) Increasing the amount of added light, the red line moves toward the origin. The pixels selected in this region of the phasor plot map to certain regions of the cytoplasm where the concentration is about 0.12mM. d) Zoomed part of panel c near the origin.

The cluster region indicated by the small red dot along the line blue-red after addition of a given amount of external light moves to the point corresponding to the intercept of the blue line with the red line. The red line position is directly proportional to the NADH concentration so that all points along the red line have the same concentration. For this position of the red line the concentration is 0.29mM. We have already identified in Fig. 4 that the selection of this cluster corresponds to pixels in the nucleus. Now we move the blue line to the other cluster that was identified with points in the cytoplasm. After adding the external light, this cluster moves to the position indicated by the red line in Fig. 6(b). Along this line the NADH concentration is 0.89mM. In Fig. 6(c) (zoomed in Fig. 6(d)) we show that there are other pixels, originally in the cytoplasm that move to a different position along the blue line. This position corresponds to a concentration of 0.12mM.

Finally, a simple software algorithm can paint the original image pixel by pixel using a color scale based on concentration rather than fluorescence intensity. This is shown in Fig. 7.

#263167 Received 14 Apr 2016; revised 19 May 2016; accepted 19 May 2016; published 1 Jun 2016

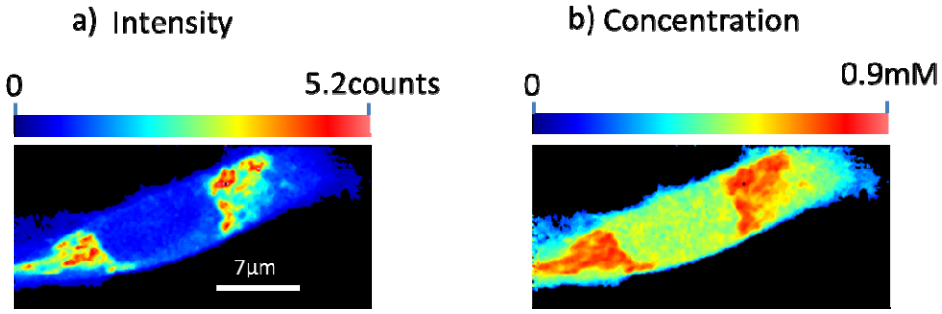

Fig. 7. a) Intensity image of NADH in a CHO-K1 cell. The color scale is in counts/pixel/frame. b) NADH concentration image according to the method described in this paper. The concentration scale was calibrated using a solution 1mM free-NADH.

5. Discussion

To calibrate for the absolute concentration of NADH in cells, we need a FLIM measurement of intensity of a known solution of free-NADH measured with the same illumination condition used for the cells. Once the FLIM image is obtained, the graphical method for the absolute determination of the NADH concentration is very rapid, automatic and provides accurate values of concentration as long as some assumptions are satisfied. *i*) The relative quantum yield of the components (free and bound NADH) must be known or it must be measured. These are the blue and red dots in Fig. 3(a) where we show the experimentally measured values. *ii*) There are no other major contributions to the fluorescence than the assumed species. *iii*) The volume of exploration (the height of the confocal slice) must be uniform across the sample.

In the case of NADH, the quantum yield could be assumed to be proportional to the lifetime of the two states (bound and free) so that they can be determined by independent measurement [31]. As discussed in the Introduction, the phasor position of free-NADH is easy to measure. For the bound NADH the phasor position could be obtained from solution experimental data by drawing a line from the phasor of the free NADH passing through the experimental data and intercepting the universal circle at the position of the bound NADH. However, given the binding constant for some of the enzymes, the concentration of the enzyme must be relatively large to favor the bound species. At high enzyme concentration we have to account for potential enzyme aggregation. This extrapolation procedure could be directly applied to data from a cell provided that the phasor distribution is mainly along a straight line, which is the case for the data shown in this work (Fig. 4(b)). The values obtained by this procedure for NADH are in the known range of typical values of NADH in cells [25]. Specifically, values reported in [25] using lifetime methods for the cytoplasm of breast cancer cells and for normal breast cells are in the range of 168 µM and 97 µM, respectively. Zhang and associates [32] estimated the NAD(P)H) concentration in the nucleus of Cos-7 cells to be in the range of 113 µM. In a recent comprehensive review of the various methods available to determine the concentration of NAD(P)H and other co-enzymes, Heikel reports values in the range of those measured in the CHO-K1 cell used as demonstration in this work [33]. Clearly, before concluding that the graphical method proposed in this paper to determine the concentration of NADH is accurate and precise, much more systems need to be measured and compared with classical biochemical methods. It is encouraging that our simple method provides concentrations in agreement with the current literature.

The graphical procedure discussed in this work could be applied to unknown samples. Consider the following situation: two fluorescent proteins have the same lifetime, which is frequently the case, so that they will be on the same spot on the universal circle in the phasor plot. If the two proteins have different brightness when we add the external light, they will

#263167 Received 14 Apr 2016; revised 19 May 2016; accepted 19 May 2016; published 1 Jun 2016

move different amounts toward the origin. From the amount of shift we could determine their relative brightness. If we know the concentration, we can determine the relative quantum yield. This situation is important for the case in which a biosensor has two states with different lifetimes and we need to know the concentration of the two species. Various research groups have discussed how this can be achieved and have developed spectral analyses to solve this problem [34–39]. Here we are suggesting that an alternative method could be the use of the FLIM method developed in this work.

When collecting a FLIM image, we are measuring the lifetime at each pixel. If there are other substances and they contribute differently in different regions of the cell, then we should be able to separate the contribution of additional species and build a graphical analysis model for 3 components instead of the two-component model used here. Note that the experimental values of the fluorescence lifetime in the cell (Fig. 6) align along the line between free and bound NADH. In the specific example discussed in this work presumably we only have the mixture of 2 components in each pixel. This is not always the case and in many experiments of cell autofluorescence using the same excitation and emission filters used in this work we observe pixels that are not along the line of linear combination of free and bound NADH [30].

For the calibration solution, the intensity is coming from the entire volume of excitation. In the case of cells, the intensity could arise only from a part of the volume of excitation. If the volumes of excitation are different then the concentration in the entire volume of excitation is average with parts that could contain more or less NADH. For example, in a thin lamella of a cell the volume of excitation could be a small section of the cell. In this case what we are measuring is the average concentration.

If strong scattering is present, such as occur in thick tissues, the fluorescence intensity will be a function of the depth in the sample but the NADH lifetime is independent of the scattering. In this case the NADH concentration must be corrected for an additional term which is due to the attenuation of the signal in the sample. This scattering term could be calibrated using a thick scattering sample for the calibrated solution. The slope of the intensity as a function of depth for the solution with added scattering could be compared to the slope of the loss of signal in the sample; hence an additional correction term could be derived.

Apart from the systematic errors discussed above, there is an error in the determination of the concentration due to the uncertainty in the determination of the intensity and the lifetime at each pixel. The errors associated with the calibration solution are minimal since 1mM NADH solution is very bright. In that phasor representation, the error in the position of the phasor from a pixel only depends on the photon collected at each pixel. In the measurements shown in this work, the counts per pixel per frame are at a level of 5.2 for the pixel with maximum intensity. Generally we collect 40 frames for a total count of about 200 in the pixel with maximum intensity. According to the expressions derived in Colyer and Gratton [40] for this count rate the uncertainty is about 5% in the position of the phasor. This uncertainty propagates to a similar uncertainty using Eq. (2) (and the corresponding equation for the s-coordinate, not used in this work). Since the uncertainty depends on the inverse of the square-root of the number of photons, a pixel with 50 counts will have twice that uncertainty [40]. If needed, we could average 3x3 pixels to reduce the uncertainty by a factor of 3.

Can this method work with time domain fluorescence decay data without using the phasor transformation? Theoretically yes. However, for every pixel we need to resolve for two (or more) exponential components and the background contribution. We have a total of 2 lifetimes (which presumably are known), 2-preexponential factors and the background term. This analysis can be difficult to perform because a small shift in the lifetime values could have a large effect on the pre-exponential factors.

We note that the only equations used for this work are the equations for linear combination of lifetime components (phasors) in the phasor plot (Eqs. (1) and (2)). A user interface for the calculation of absolute concentrations of NADH in cells is available in the SimFCS software at www.lfd.uci.edu\software.

#263167 Received 14 Apr 2016; revised 19 May 2016; accepted 19 May 2016; published 1 Jun 2016

6. Materials and methods

Cells preparation. Chinese hamster ovary (CHO-K1) cells were cultured and maintained in a 37°C incubator humidified at 5% CO2 atmosphere in Dulbecco's modified Eagle's medium/F12(D-MEM) (1:1) (11320-033, Life Technologies, Carlsbad, CA), supplemented with 10% fetal bovine serum and 1% penicillin streptomycin. The cells were freshly trypsinized and plated onto 35 mm glass bottom dishes (Mattek Corporation, Ashland, Massachusetts) for imaging.

Microscopy. The phasor FLIM images were acquired with LFD customized microscopy system M3 which is a modified Zeiss Axiovert S100TV microscope(Carl Zeiss, Jena, Germany) coupled with a two-photon Ti: Sapphire laser(Spectra-Physics MaiTai) and Becker&Hickl SPC-830 card(Becker and Hickl, Berlin). A Zeiss 40x1.2 NA water immersion objective (Carl Zeiss, Oberkochen, Germany) is used. The specimens were excited at 740nm and the emission signal is split with 496nm dichroic filter and detected in two channels using a band pass filter 460/40 nm and a band pass filter at 540/50-565nm for the second channel. Only the blue channel was used in this study.

Free NADH preparation. For pure free NADH FLIM calibration, NADH (Sigma N8129) were diluted in 10X Tris-HCL buffer (pH = 7.4).

Sample preparation to lifetime measurements of NADH bound to Lactate Dehydrogenase

Powder L-Lactic Dehydrogenase (LDH) from rabbit muscle (code L1254, Sigma-Aldrich, Inc) was prepared in buffer Tris-HCl 0.2 mM, pH 7.5. Later the enzyme was cleaned for whatever contaminant using Vivaspin 2 Centrifugal Concentrator (GE Healthcare). Following the specification of the manufacturer we changed the same buffer 5 times. After the concentration protocol the supernatant was centrifuged for 20 minutes at 9500 xg in order to remove precipitations. The amount of protein was determined using absorbance at 280nm with an extinction coefficient of 205000 $M^{-1}.cm^{-1}$ [31] in a NanoDrop 2000 UV-Vis Spectrophotometer (Thermo Fisher Scientific Inc). A final concentration of enzyme around 22 μM were reached, the enzyme was used immediately or stored in the refrigerator at 4°C for 1 week. The β-Nicotinamide adenine dinucleotide (NADH, 10107735001 ROCHE, Sigma-Aldrich, Inc) was prepared fresh every day as stock solution of 250 μM in a Tris-HCl buffer 0.2 mM, pH 7.5, the absolute concentration of the NADH was determined measuring the absorbance of 340 nm using an extinction coefficient 6200 $M^{-1}.cm^{-1}$ [31], with a Perkin-Elmer Lambda 40 spectrophotometer. Following the thermodynamic reversible equilibrium rules for the enzyme /ligand complexation [41], we determined the percentage of enzyme/ligand complex (EL) using the described dissociation constant (K_D) equal to 0.2 μM [31] in 100 mM of the oxalic acid (75688 Sigma-Aldrich, Inc). An approximate ratio of 92.7% of EL was prepared by the incubation at room temperature for 30 min of 2.2 μM of LDH and 0.05 μM of NADH (see Eqs. (3), (4), and (5)). Consider to following equilibrium E + L ⇔ EL where E, L and EL represent: the free enzyme, free ligand and EL complex at the equilibrium, respectively and the rate of dissociation

$$K_D = \frac{[E][L]}{[EL]} \tag{3}$$

Using the initial concentration of the E_0 (E_0 = E-EL) and L_0 (L_0 = L-EL) and reorganizing the terms in the K_D expression it is possible to obtain the follow notation for the EL equilibrium concentration.

$$[EL] = \frac{(K_D + E_0 + L_0) - \sqrt{\left[(K_D + E_0 + L_o)^2 - 4E_0L_0\right]}}{2} \tag{4}$$

#263167 Received 14 Apr 2016; revised 19 May 2016; accepted 19 May 2016; published 1 Jun 2016

and the EL percentage as:

$$EL\% = \left(\frac{[\mathrm{EL}]}{[\mathrm{E}]} \right) * 100 \tag{5}$$

The FLIM measurements were taken in an Olympus FluoView FV1000 system with IX81 microscope and 2-photon excitation of 740 nm using a Spectra-Physics MaiTai HP laser and Fast-FILM-box (ISS, Inc). For the NADH lifetime measurement we used a water immersion UPL SAPO Olympus objective 60x with a NA 1.2 and a filter block composed of two band pass filter of 460/40 nm and 540/50 nm with a dichroic mirror 495 nm longpass filter The calibration of the system was performed using a solution of 10 μM of Rhodamine 110, with a lifetime of 4.0 ns (ISS webpage at www.iss.com).

Acknowledgments

This work was supported in part by grants form National Institute of General Medical Sciences 100000057 P41-GM103540 and P50-GM076516 (MAD, LM and EG); California Institute for Regenerative Medicine 100000900 RB5-07458 (NM).